

Supporting Information

Unusually large fluorescence quantum yield for a near-infrared emitting DNA-stabilized silver nanocluster.

Vlad A. Neacșu,^{a,†} Cecilia Cerretani,^{a,†} Mikkel B. Liisberg,^a Steven M. Swasey,^b Elisabeth G. Gwinn,^c Stacy M. Copp,^{d,e} and Tom Vosch^{a,*}

^a Nanoscience Center and Department of Chemistry, University of Copenhagen, Universitetsparken 5, 2100 Copenhagen, Denmark. Email: tom@chem.ku.dk

^b Department of Chemistry, University of California, Santa Barbara, Santa Barbara, California 93106, United States.

^c Department of Physics, University of California, Santa Barbara, Santa Barbara, California 93106, United States.

^d Department of Materials Science and Engineering, University of California, Irvine, Irvine, California 92697-2585, United States.

^e Department of Physics and Astronomy, University of California, Irvine, Irvine, California 92697-4575, United States.

[†] Both authors contributed equally.

Materials and methods

Sample preparation

The oligonucleotide (5'-CCCGGAGAAG-3') was purchased from IDT. Silver nitrate (AgNO_3 , $\geq 99.998\%$) and sodium borohydride (NaBH_4 , 99.99%) were purchased from Sigma Aldrich. All chemicals were used as received. All solutions were prepared in nuclease-free water (IDT).

The DNA-AgNCs were synthesized by mixing the hydrated DNA with AgNO_3 in a 10 mM ammonium acetate (NH_4OAc) solution. After 15 minutes, NaBH_4 was added in order to reduce the silver cations. The ratio of the components in the final mixture was $[\text{DNA}]:[\text{Ag}^+]:[\text{BH}_4^-] = 1:5:2.5$. The optimal concentration of DNA to get the highest reaction yield was found to be 20 μM .

Kinetics of formation

In order to ensure the highest reaction yield, the evolution of the fluorescence intensity at 720 nm (emission maximum) was recorded as a function of time for 24 hours. The excitation source was an LDH-P-635 pulsed laser from Picoquant ($\lambda_{\text{exc}} = 634.8$ nm). Based on the curve (Figure S1),

we fitted and extrapolated the data with a growth function ($f(x) = \frac{ax}{b+x}$) to calculate the time needed to reach the plateau (defined as the point in time where the increase in intensity is less than 0.1%). The result of the extrapolation indicated that 114 hours were needed in order to maximize the formation yield of the DNA-AgNCs, therefore the sample was kept in the fridge for five days before purification.

HPLC purification

The HPLC purification was performed using a preparative HPLC system from Agilent Technologies with an Agilent Technologies 1260 Infinity fluorescence detector and Agilent Technologies 1100 Series UV-Vis detector, and a Kinetex C18 column (5 μm , 100 \AA , 50 \times 4.6 mm), equipped with a fraction collector. The mobile phase was a gradient mixture of 35 mM triethylammonium acetate (TEAA) buffer in water (A) and methanol (B). The gradient was varied from 12% to 95% B as follows: 0-2 min 12% B, 2-17 min linear increase of B until 27%, 17-20 min from 27% to 95% B. The run was followed by 2 minutes of washing with 95% B to remove any traces of the sample from the column. The flow rate was 1 mL/min. Based on the chromatograms (Figure S2), a single fraction with a retention time around 12 minutes ($\sim 22\%$ B) was collected by using the absorbance signal at 645 nm.

After purification, the solvent was exchanged to 10 mM NH_4OAc by spin-filtration (cut-off = 3 kDa) in order to increase the stability of the sample over time.

Absorption and steady-state emission measurements

All absorption measurements were carried out on a Cary 300 UV-Vis spectrophotometer from Agilent Technologies using a deuterium lamp for ultraviolet radiation and a tungsten-halogen lamp for visible and near-infrared radiation.

Steady-state fluorescence measurements were performed using a FluoTime300 instrument from PicoQuant, exciting at 637.8 nm with a pulsed laser (LDH-P-C-640B). The 2D emission vs excitation plot was acquired with the same instrument using a Xenon arc lamp as excitation source. All emission spectra have been corrected for the wavelength dependency of the detector, and the 2D plot was additionally corrected for the lamp power.

Temperature-dependent emission intensity

The temperature-dependent emission trace between 10 °C and 40 °C was constructed by recording the fluorescence intensity at the emission maximum (720 nm) every 2 °C. The measurements were performed using a FluoTime300 instrument (PicoQuant) and exciting at 634.8 nm with an LDH-P-635 pulsed laser. In order to account for the variations in laser intensity, each point was measured 50 times with 1 second interval. The software only provided the final average value, which was plotted.

The temperature-dependent emission trace between 5 °C and 30 °C was constructed by recording the fluorescence spectra in the interval 650 nm – 800 nm every 5 °C. The measurements were performed using a FluoTime300 instrument (PicoQuant) and exciting at 637.8 nm with an LDH-P-C-640B pulsed laser. At the same time, the laser power of the transmitted beam was recorded using a power meter (Thorlabs). Each emission spectrum was normalized by the average laser power during the recording of the spectrum. The emission intensity at 720 nm was plotted as a function of temperature. Since it is a single intensity value, no error is available.

In both cases, in order to ensure thermal equilibrium at each temperature, every measurement was carried out 20 minutes after the target temperature had been reached. The excitation source was blocked between measurements.

Quantum yield determination

Quantum yield was determined through a relative method, using a terrylene diimide (TDI) in toluene ($Q_R = 0.69$) as reference.¹ No error was provided on this reference value. The absorption and emission spectra were recorded at different concentrations for the sample and the reference. The integrated emission spectra were then plotted as a function of the fraction of absorbed light at the excitation wavelength ($f = 1 - 10^{-A}$). The data was fitted linearly while fixing the y-intercept at zero, and the slope was used to calculate the quantum yield based on the following equation:

$$Q_S = Q_R \cdot \left(\frac{\alpha_S}{\alpha_R} \right) \cdot \left(\frac{n_S^2}{n_R^2} \right)$$

where S and R stand for the sample and reference, respectively, Q is the quantum yield, α is the slope of the linear regression and n is the refractive index of the solvent.

We can assume that the refractive indices of the solvents ($n_{\text{water}} = 1.3325$ and $n_{\text{toluene}} = 1.497$) bear no significant error. Propagating the errors of the slopes and the reference's quantum yield, the error of the sample's quantum yield is:

$$\sigma_{Q_S}^2 = \sigma_{Q_R}^2 \cdot \left(\frac{\alpha_S}{\alpha_R} \left(\frac{n_S}{n_R} \right)^2 \right)^2 + \sigma_{\alpha_S}^2 \cdot \left(\frac{Q_R}{\alpha_R} \left(\frac{n_S}{n_R} \right)^2 \right)^2 + \sigma_{\alpha_R}^2 \cdot \left(-Q_R \cdot \alpha_S \cdot \frac{1}{\alpha_R^2} \left(\frac{n_S}{n_R} \right)^2 \right)^2$$

Knowing the values:

$$Q_R = 0.69, \alpha_S = 4.98277 \cdot 10^8, \alpha_R = 3.72677 \cdot 10^8, \sigma_{\alpha_S} = 5.35121 \cdot 10^6, \sigma_{\alpha_R} = 3.13868 \cdot 10^6$$

And replacing everything, we obtain:

$$\sigma_{Q_S}^2 = \sigma_{Q_R}^2 \cdot 1.122169 + 6.16196 \cdot 10^{-5} + 3.78953 \cdot 10^{-5}$$

Depending on the values of the error on the reference's quantum yield, the error on our sample's quantum yield can be:

σ_{QR}	0	0.01	0.02	0.04	0.05	0.08	0.1	0.15	0.2
σ_{QS}	0.00998	0.01455	0.02342	0.04353	0.05390	0.08533	0.1064	0.1592	0.2121

From the table above, it is easy to see that the main contribution to the error of our quantum yield is attributed to the error on the reference's quantum yield, therefore we can say that the error on our quantum yield is similar to the error on the reference's quantum yield.

Time-Correlated Single Photon Counting (TCSPC)

Time-resolved fluorescence and anisotropy measurements were conducted using a FluoTime300 instrument from PicoQuant with a 637.8 nm pulsed laser (LDH-P-C-640B) as excitation source for all experiments. The data has been analyzed using FluoFit v.4.6 software from PicoQuant.

Time-resolved emission spectra (TRES) were constructed by measuring fluorescence decays in the interval 660 nm–800 nm, in steps of 5 nm, with an integration time of 30 seconds for every decay, in order to acquire at least 10 000 counts in the maximum at the emission maximum.

Low-Temperature Measurements

Low-temperature measurements were performed in liquid nitrogen (-196 °C), and in a mixture of dry ice (solid CO₂) and acetone (-78 °C). In order to limit the influence of the scattering from the ice, two filters were employed during these measurements: a 640 nm band-pass filter (LD01-640/8-25, Semrock) in the excitation path, and a 647 nm long-pass filter (BLP01-647R-25, Semrock) in the emission path. All decay curves at -196 °C were globally fitted with a tri-exponential reconvolution model including the instrument response function (IRF), while at -78 °C a bi-exponential reconvolution model with the IRF was used.

Acquisition and analysis of TRES data

All decay curves were globally fitted with mono- and bi-exponential reconvolution models including the IRF. The obtained spectra were corrected for the detector efficiency and transformed to wavenumber units by multiplying with the Jacobian factor ($10^7 / \nu^2$). The spectra were interpolated with a spline function using the built-in `spaps` MATLAB function with a tolerance of 10^{-10} (forcing the interpolated curve to go through the data points). The wavenumber step of the interpolation was equivalent to 0.001 nm wavelength. The emission maxima were taken as the maxima of the interpolated TRES. The average decay time $\langle \tau \rangle$ of every decay was calculated as the intensity-weighted average lifetime. The intensity-weighted lifetime $\langle \tau_w \rangle$ was calculated as the average of $\langle \tau \rangle$ over the emission spectra weighted by the steady-state intensity.

Acquisition and analysis of time-resolved anisotropy data

Time-resolved anisotropy measurements were performed by exciting the sample with vertically polarized light using a 637.8 nm pulsed laser (LDH-P-C-640B). The vertically and horizontally polarized fluorescence intensity decays were recorded. All decays were fitted with FluoFit v 4.6 from PicoQuant using a mono-exponential reconvolution model for both the lifetime and the rotational correlation time (θ). The anisotropy was measured at six different temperatures (5 °C, 10 °C, 15 °C, 20 °C, 25 °C, 30 °C) and the hydrodynamic volume of the cluster was calculated using the Perrin equation:

$$\theta = \frac{\eta V}{k_B T}$$

where η is the dynamic viscosity of the solvent, V is the hydrodynamic volume of the species (assumed to be spherical), k_B is the Boltzmann constant and T is the absolute temperature. Additional information about the Perrin equation and the determination of the hydrodynamic volume can be found in Principles of Fluorescence Spectroscopy.²

OADF and UCF measurements

Optically activated delayed fluorescence (OADF) measurements were conducted on a home-built confocal microscope. A continuum white-light laser (NKT Photonics, SuperK EXTREME EXB-6) operating at 11 MHz was used as an excitation source, providing wavelengths in the range of 420 to 2400 nm. This broad band output was initially divided into two paths by a 650 nm long pass dichroic mirror (Thorlabs, DMLP650R), yielding a primary beam with wavelengths below 650 nm and a secondary beam with wavelengths above 650 nm. The primary beam was cleaned up with a 640 nm band pass filter (Semrock, LD01-640/8). The secondary beam was coupled into a 10 m polarization maintaining fiber (Thorlabs, P1-780PM-FC-10) used to generate a delay between the two beams. The secondary beam was subsequently cleaned up with an 810 nm band-pass filter (Chroma, ET810/90m) and a tunable long pass filter (Semrock, TLP01-790 – set at an angle of approximately 29°). Both beams were then co-aligned by a 650 nm long-pass dichroic mirror (Thorlabs, DMLP650R). Further cleaning of the combined beams was assured by a 561 nm long pass filter (Semrock, BLP01-561), 633 nm long pass filter (Semrock, LP02-633RU), and 950 nm short pass filter (FF01-950/SP).

The combined beams were then reflected with a 30:70 beam splitter (Omega Optical, XF122) into an oil-immersion objective (Olympus, UPlanSApo 100x, NA = 1.4). The objective focused both beams onto the sample and collected the fluorescence. The fluorescence was directed through a 100 μ m pinhole and was separated from the laser light of the primary and secondary beams by a combination of the following filters: 647 nm long-pass filter (Semrock, BLP01-647), 700 nm short-pass filter (Chroma, ET-700SP-2P8), 750 nm short-pass filter (Semrock, FF01-750/SP), and 710 nm band-pass filter (Chroma, ET710/75x). Lifetime measurements were acquired with an avalanche photodiode (Perkin-Elmer, CD3226) connected to a single photon counting module (Becker & Hickl, SPC-830). Spectra were recorded by directing the fluorescence, with a flip mirror, to a spectrograph (Acton Research, SP 2356 spectrometer, 300 grooves/mm) onto a nitrogen cooled CCD camera (Princeton Instruments, SPEC-10:100B/LN-eXcelon). No spectral correction was applied on the recorded spectra. In order to determine the OADF contribution to the secondary fluorescence (SF) in Figure 4B, the integrated area of the UCF only signal (see Figure S8) was subtracted from the integrated area of the SF from Figure 4B. Both the OADF and UCF signals were then divided by the integrated area of the primary fluorescence (PF, see Figure 4B).

Fitting the OADF contribution in Figure 4A with a growth function ($f(x) = \frac{ax}{b+x}$) yielded a maximum value of 4.3% (fit not shown), which represents the minimum Q_{D1} value. See supporting information of Krause *et al.* for a detailed explanation of why this is the minimum Q_{D1} value.³

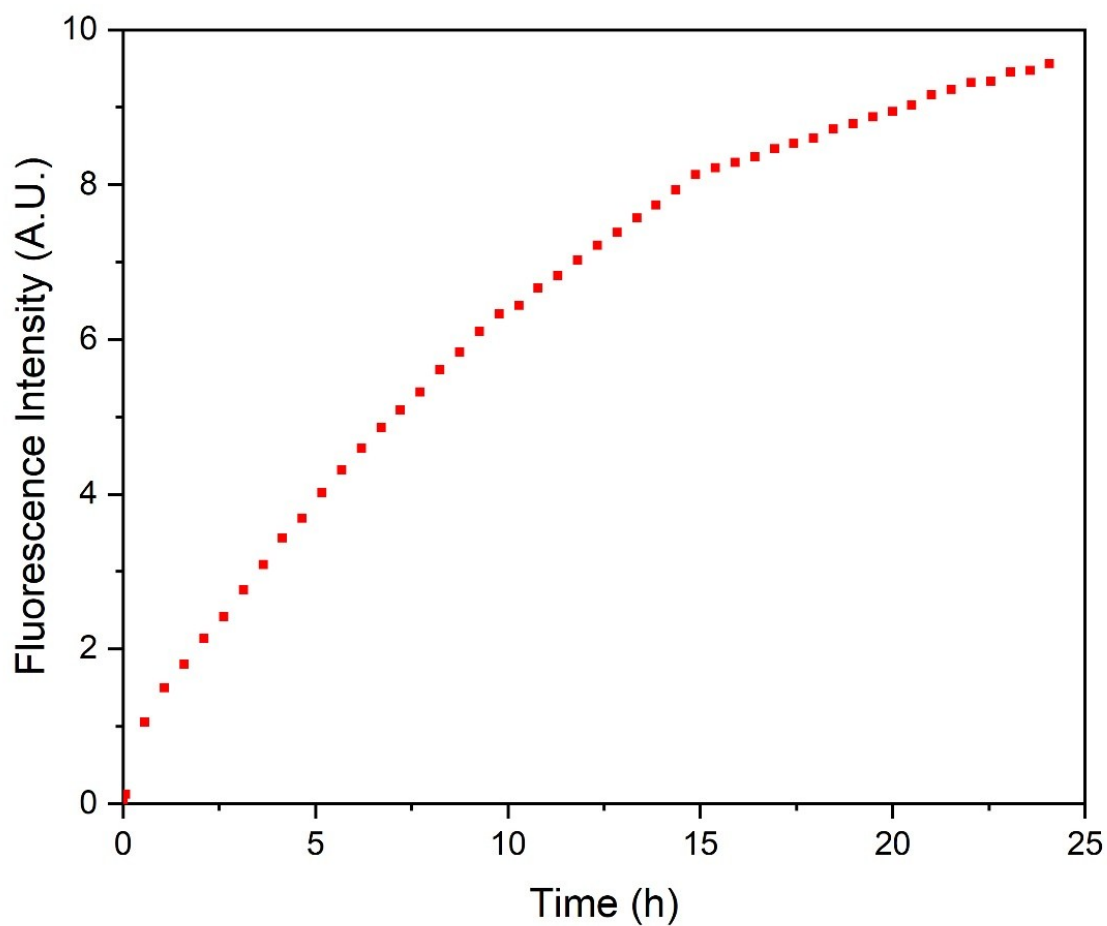


Figure S1. Formation curve of DNA-AgNCs in 10 mM NH_4OAc at room temperature. After the synthesis of the DNA-AgNCs, the emission intensity at 720 nm was measured every 30 minutes (starting 4 minutes after synthesis), exciting at 634.8 nm (LDH-P-635) in order to follow the formation of the emissive species. The plot shows the fluorescence intensity as a function of time after synthesis. The measurement was started 4 minutes after the addition of the reducing agent, NaBH_4 , and the sample was stirred for the duration of the experiment. Moreover, the laser source was blocked between measurements.

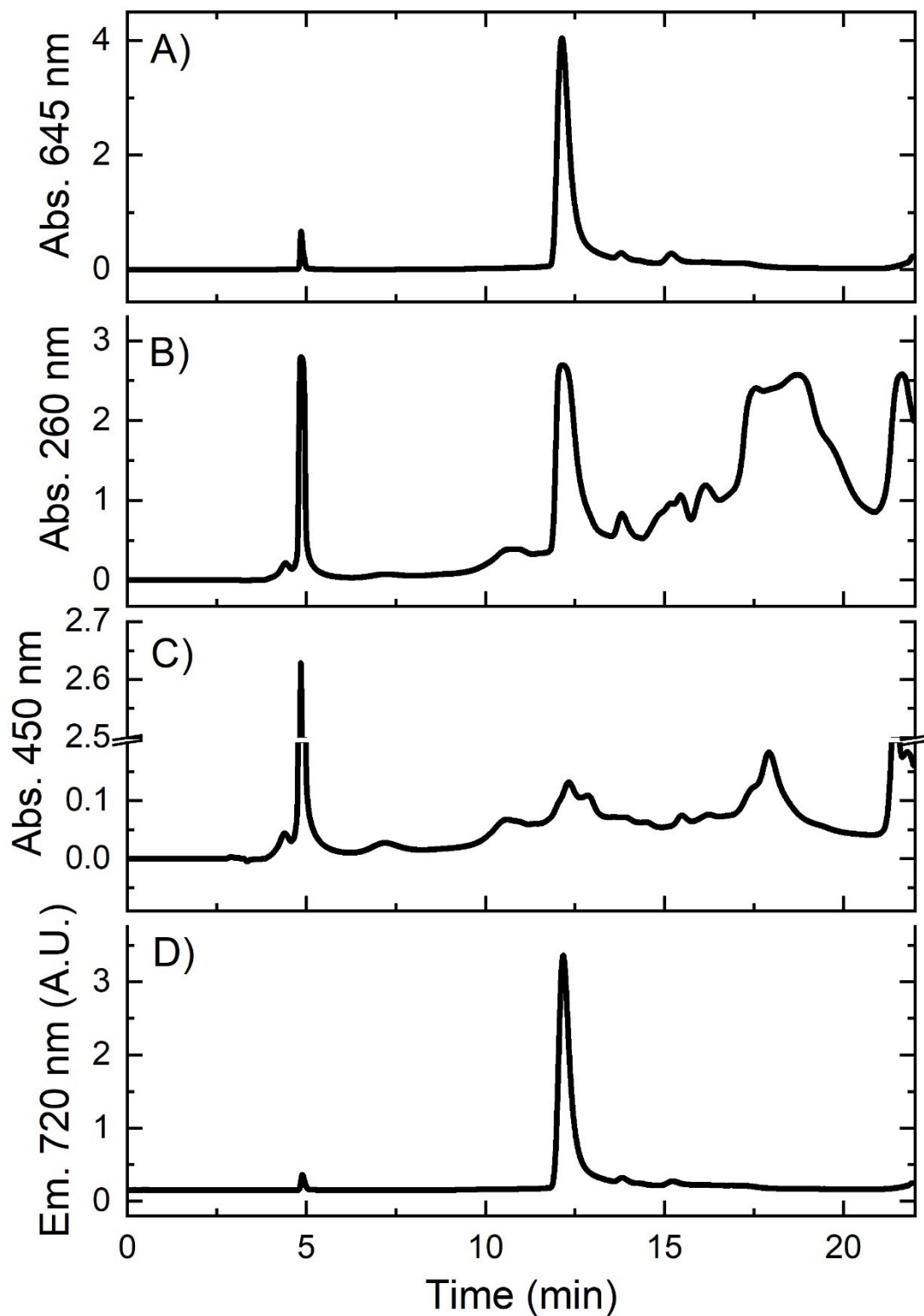


Figure S2. HPLC chromatograms of DNA-AgNCs **A)** monitoring the absorption of the clusters at 645 nm; **B)** monitoring the absorption of the DNA at 260 nm; **C)** monitoring the plasmon absorption of the silver particles at 450 nm; and **D)** monitoring the emission of the clusters at 720 nm (exciting at 645 nm). The fraction collected at ~12 min is the sample described in the manuscript.

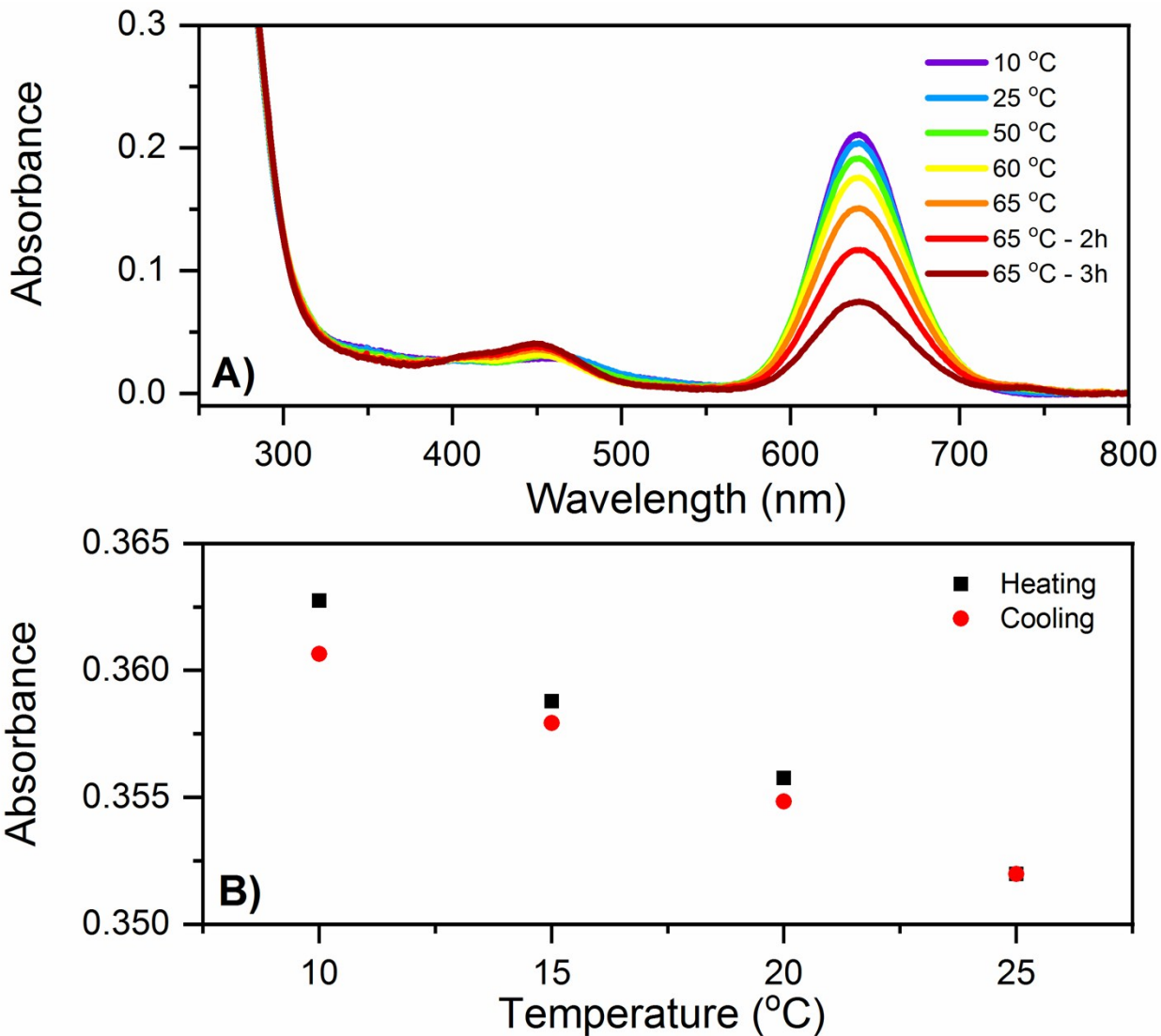


Figure S3. A) Absorption spectra of DNA-AgNCs in 10 mM NH₄OAc at different temperatures. At each temperature, the sample was kept for approximately one hour in order to ensure thermal equilibrium. The last three spectra were measured after keeping the sample at 65 °C for 1, 2, and 3 hours, respectively. **B)** Absorbance of DNA-AgNCs in 10 mM NH₄OAc at 640 nm as a function of temperature during a heating-cooling cycle. The sample was kept for 10 minutes at every temperature in order to ensure thermal equilibrium.

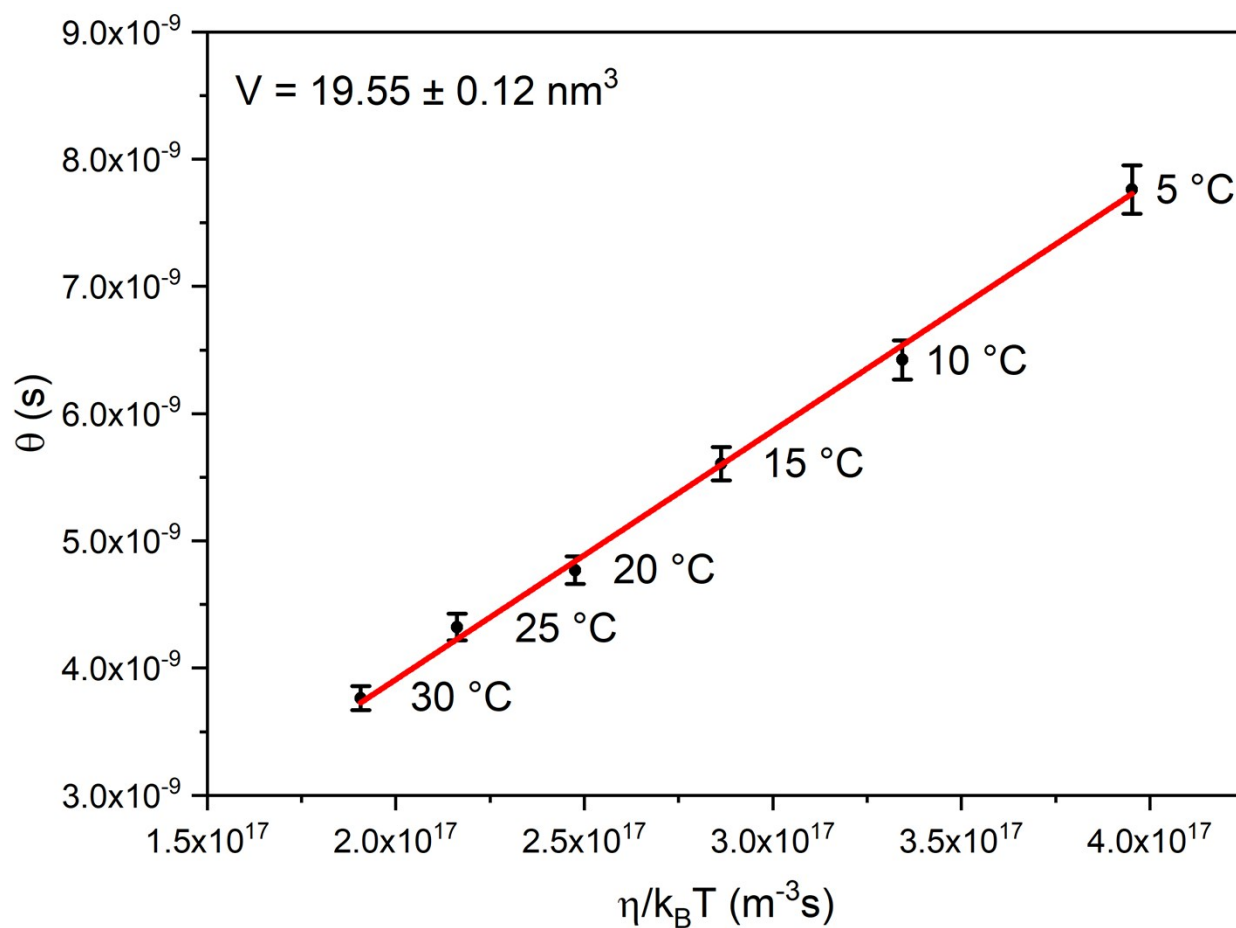


Figure S4. Linear fit of the rotational correlation times (θ) as a function of $\eta/k_B T$ for DNA-AgNCs in 10 mM NH_4OAc . The slope (V) represents the hydrodynamic volume. The individual time-resolved anisotropy decays, used to determine θ , can be found in Figure S10.

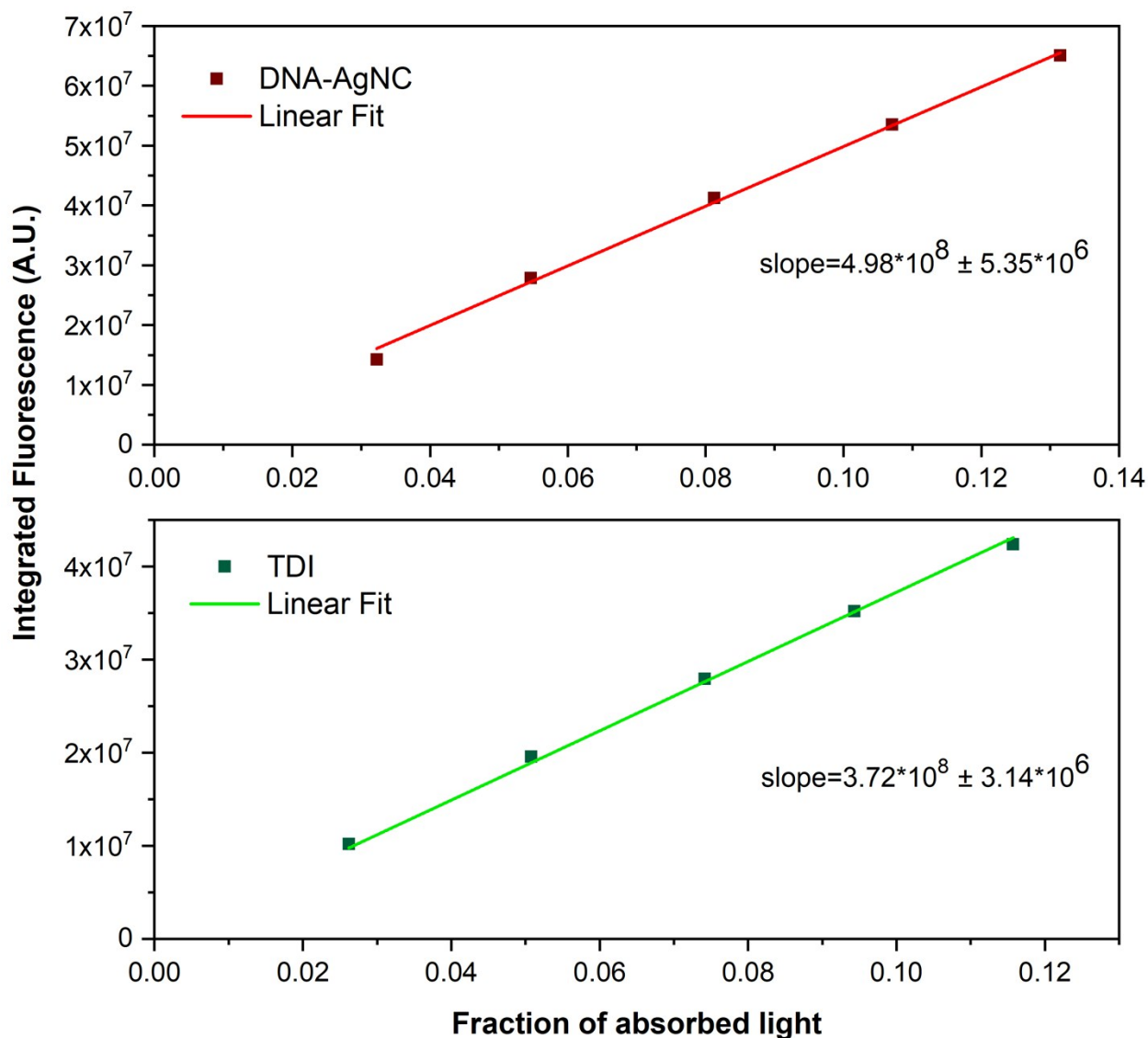


Figure S5. Zero-intercept linear fits of the integrated fluorescence counts plotted against the fraction of absorbed light for DNA-AgNCs (in 10 mM NH₄OAc) and TDI (in toluene) at 25 °C. The resulting slopes were used to determine the fluorescence quantum yield. The standard error on the slope is also provided. The fraction of absorbed light is defined as $f = 1 - 10^{-A}$, where A is the absorbance at the excitation wavelength. The individual spectra collected to make these graphs can be found in Figure S9.

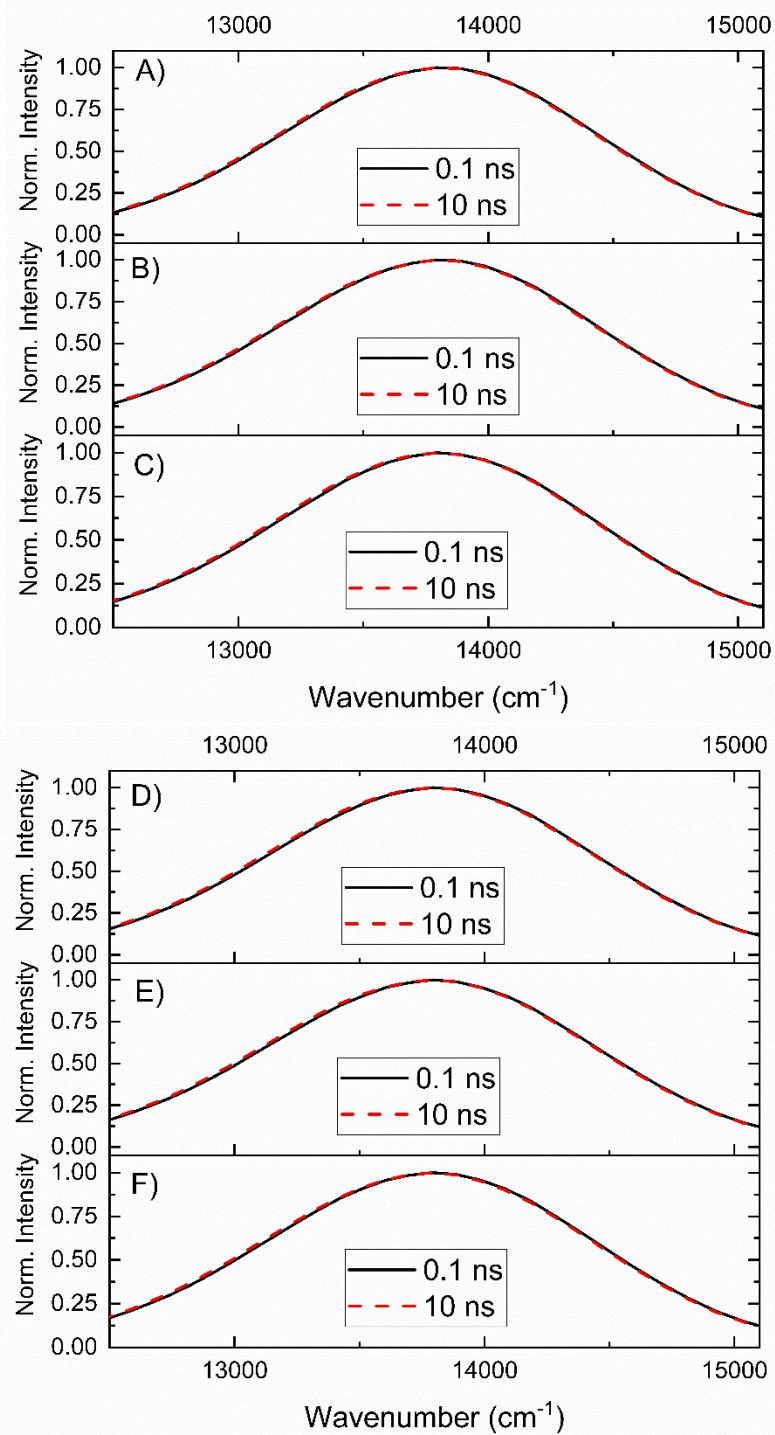


Figure S6. Time-resolved emission spectra (TRES) of DNA-AgNCs in 10 mM NH_4OAc at **A)** 5 °C, **B)** 10 °C, **C)** 15 °C, **D)** 20 °C, **E)** 25 °C, and **F)** 30 °C.

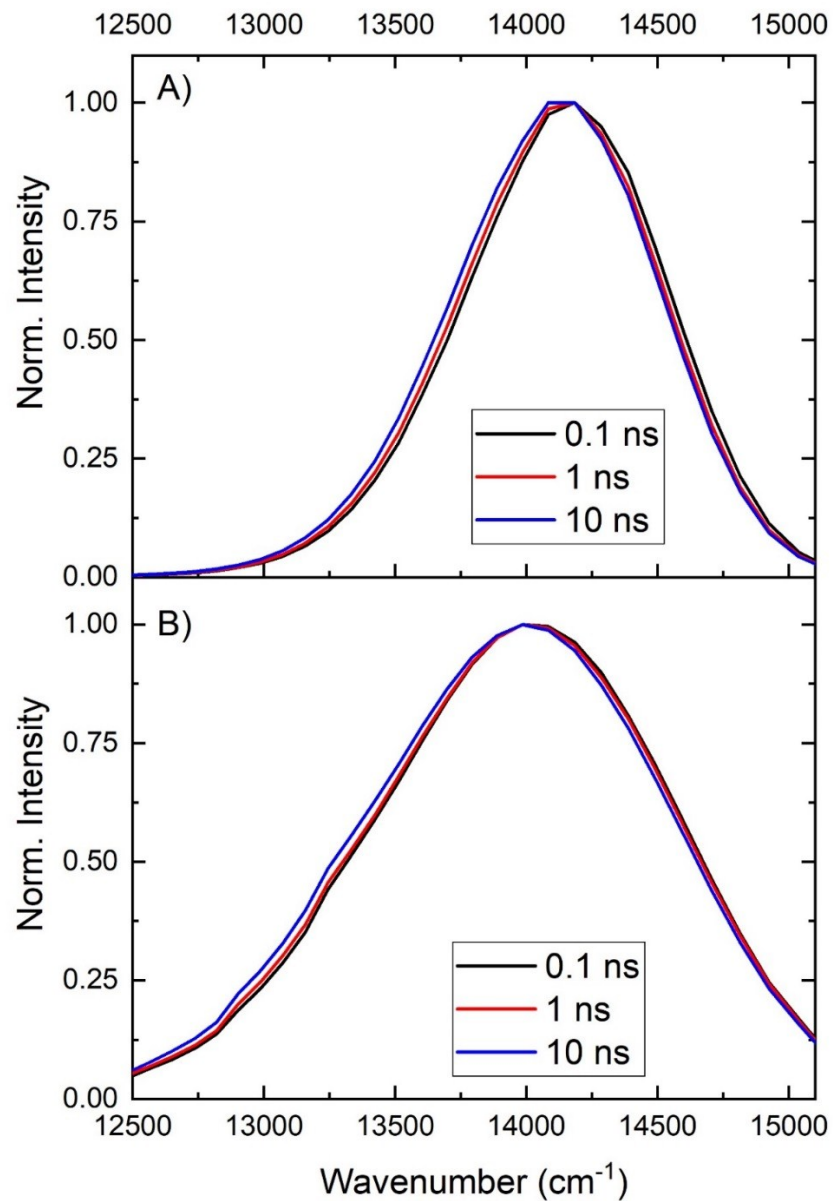


Figure S7. Time-resolved emission spectra (TRES) of DNA-AgNCs in 10 mM NH₄OAc **A)** at -196 °C, and **B)** at -78 °C.

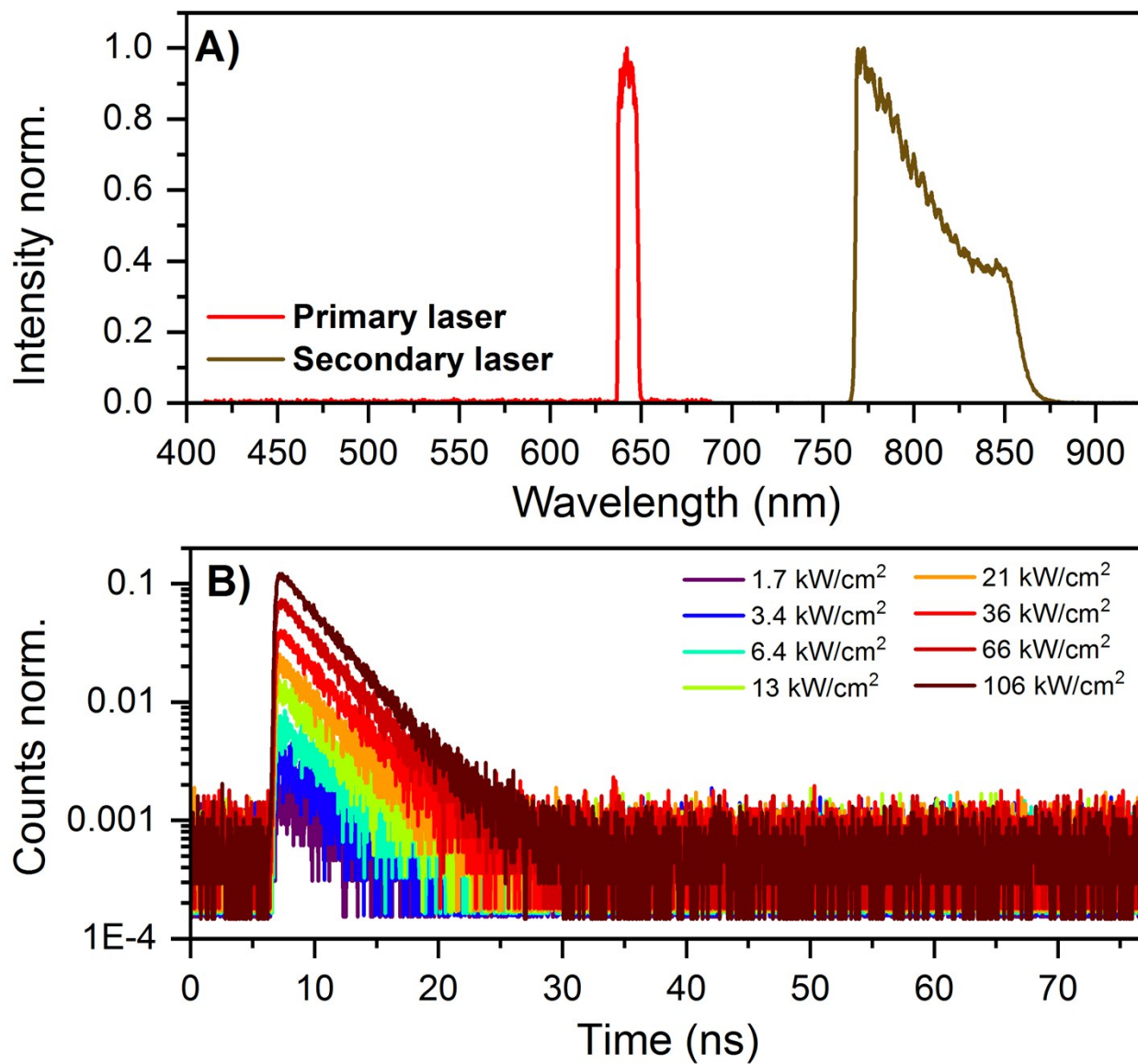


Figure S8. **A)** Primary and secondary laser profiles for the OADF experiments. **B)** Secondary fluorescence decays at different power intensities.

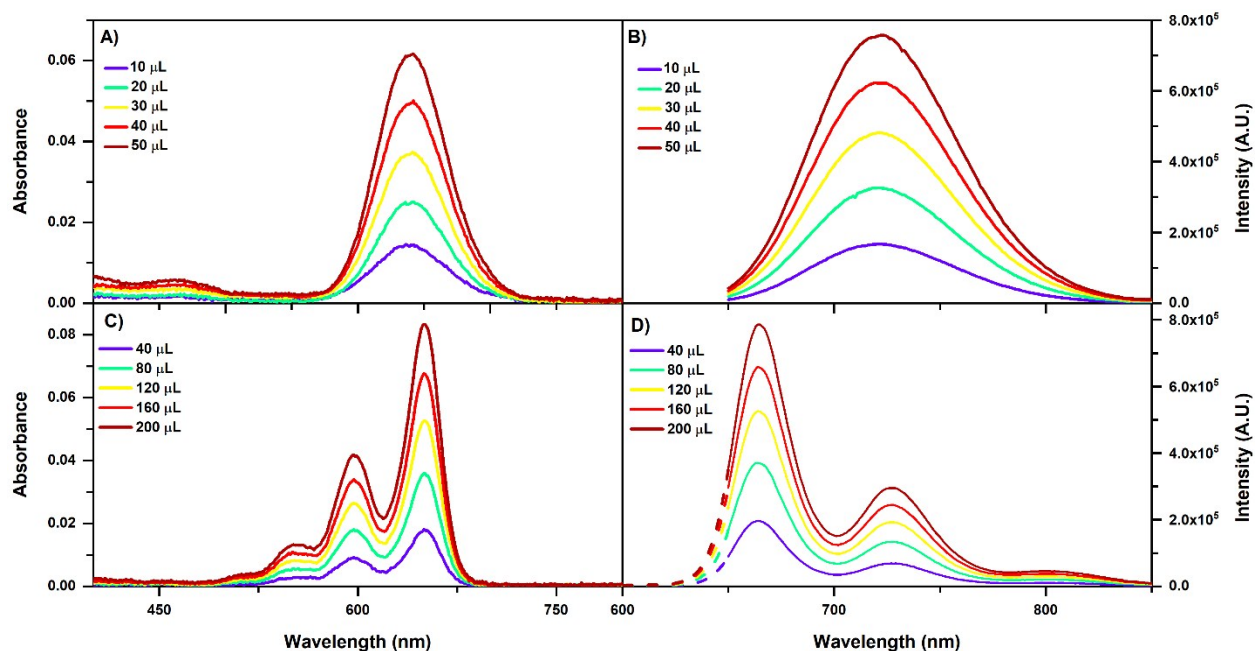


Figure S9. A,C) Absorption and **B,D)** emission spectra of DNA-AgNCs in 10 mM NH_4OAc and Terrylene diimide (TDI) in toluene, respectively. The spectra acquired at 25 °C correspond to consecutive additions of DNA-AgNCs and TDI and were used to calculate the quantum yield of DNA-AgNCs in Figure S5. The emission spectra were recorded from 650 nm by exciting with a 637.8 nm laser (LDH-P-C-640B). The missing part of the TDI spectra was added by using the shape of an emission spectrum excited at 590 nm (Xe arc lamp). The dashed lines in D) indicate the corrections. This was not done in B) for the DNA-AgNCs since the amount of emission below 650 nm is negligible.

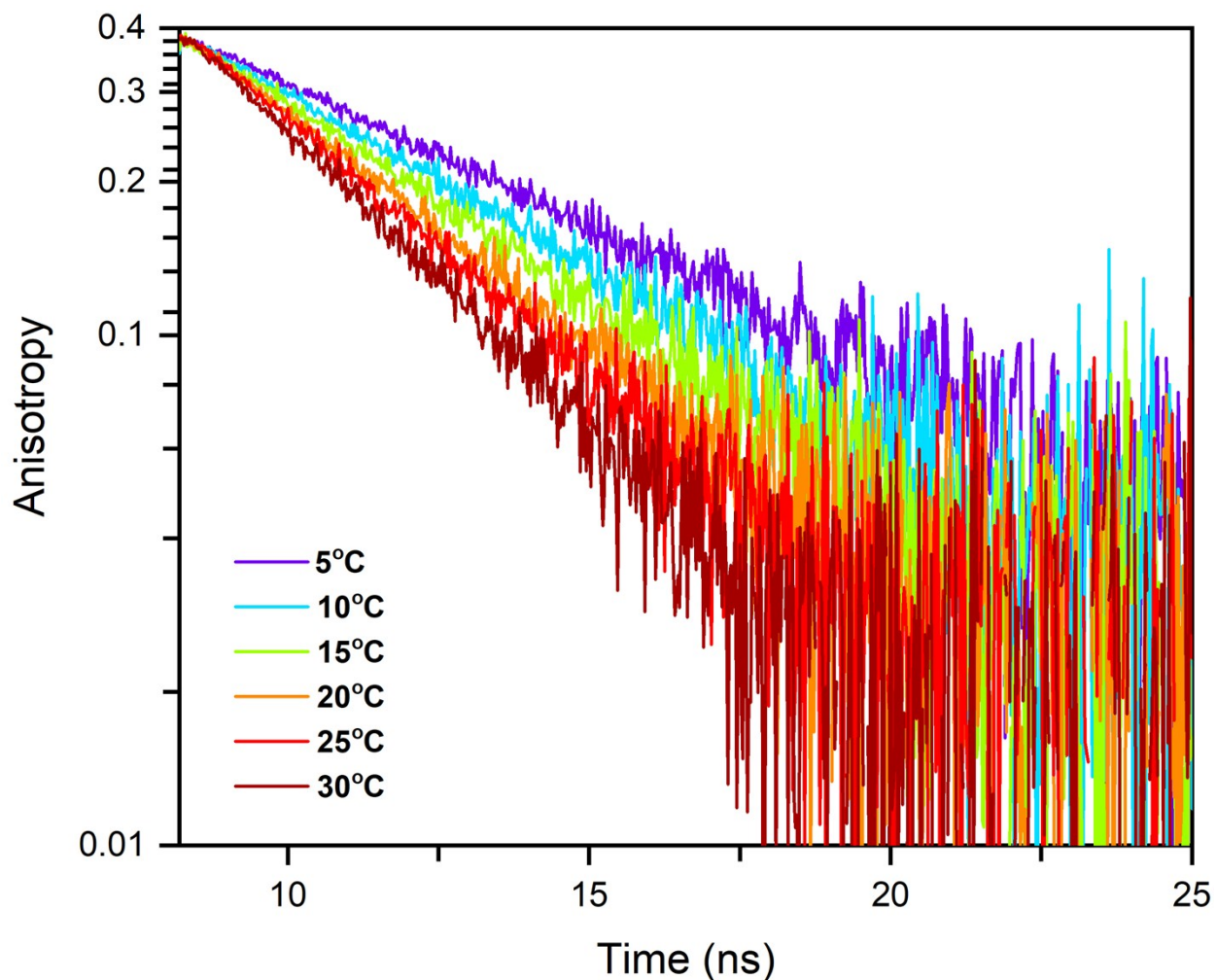


Figure S10. Time-resolved anisotropy data for DNA-AgNCs in 10 mM NH_4OAc at 5 °C, 10 °C, 15 °C, 20 °C, 25 °C, and 30 °C. The sample was excited with a vertically polarized 637.8 nm pulsed laser (LDH-P-C-640B). Rotational correlation times at different temperatures were obtained by fitting the decays. The rotational correlation times were then used to calculate the hydrodynamic volume in Figure S4.

TCSPC fits.

Table S1. Decay times and anisotropy fits of DNA-AgNCs in 10 mM NH_4OAc at different temperatures. I_x is the fractional intensity of the corresponding decay component τ_x at the emission maximum, θ is the rotational correlation time and $\langle\tau_w\rangle$ is the average decay time, weighted by the intensity over the whole emission range.

	T (°C)	Model	τ_1 (ns)	I_1 (%)	τ_2 (ns)	I_2 (%)	τ_3 (ns)	I_3 (%)	$\langle\tau_w\rangle$ (ns)	χ^2
Magic Angle	-196	3 exp.	3.82	78.24	2.85	21.65	0.47	0.11	3.63	0.91
	-78	3 exp.	3.88	88.15	2.60	11.43	0.63	0.42	3.74	0.94
	5	1 exp.	3.75	100	-	-	-	-	3.75	1.05

(Global Data Fit)	10	2 exp.	3.77	98.59	1.77	1.41	-	-	3.75	0.97	
		1 exp.	3.74	100	-	-	-	-	3.74	1.06	
	15	2 exp.	3.77	98.02	1.97	1.98	-	-	3.74	0.98	
		1 exp.	3.73	100	-	-	-	-	3.73	1.04	
	20	2 exp.	3.76	98.52	1.78	1.48	-	-	3.74	0.96	
		1 exp.	3.73	100	-	-	-	-	3.73	1.07	
	25	2 exp.	3.77	97.71	1.92	2.29	-	-	3.73	0.96	
		1 exp.	3.72	100	-	-	-	-	3.72	1.07	
	30	2 exp.	3.76	97.97	1.84	2.03	-	-	3.72	0.97	
		1 exp.	3.71	100	-	-	-	-	3.71	1.07	
	Anisotropy	T (°C)	Model	θ (ns)	χ^2						
		5	1 exp.	7.76	0.99						
		10	1 exp.	6.42	1.02						
		15	1 exp.	5.61	1.00						
20		1 exp.	4.77	0.97							
25		1 exp.	4.32	0.93							
30		1 exp.	3.76	0.98							

Table S2. Error values on the single exponential fits of the fluorescence decay time and the rotational correlation time θ in Table S1

T (°C)	τ (ns)	Error (ns)
5	3.74797	± 0.00848
10	3.73875	± 0.00850
15	3.73256	± 0.00849
20	3.72768	± 0.00880
25	3.71972	± 0.00881
30	3.71355	± 0.00890
T (°C)	θ (ns)	Error (ns)
5	7.761	± 0.189
10	6.422	± 0.153
15	5.606	± 0.132
20	4.769	± 0.109
25	4.322	± 0.105
30	3.7639	± 0.0953

References.

1. K. Kennes, Y. Baeten, T. Vosch, W. Sempels, S. Yordanov, S. Stappert, L. Chen, K. Müllen, J. Hofkens, M. Van der Auweraer and E. Fron, *J. Phys. Chem. B*, 2014, **118**, 14662-14674.
2. J. R. Lakowicz, *Principles of Fluorescence Spectroscopy*, Springer, 3rd edn., 2006.
3. S. Krause, C. Cerretani and T. Vosch, *Chemical Science*, 2019, **10**, 5326-5331.